

Vibration Performance, Stability and Energy Transfer of Wind Turbine Tower via Pd Controller

Y. S. Hamed^{1,2,*}, Ayman A. Aly^{3,4}, B. Saleh^{3,4}, Ageel F. Alogla³, Awad M. Aljuaid³ and Mosleh M. Alharthi⁵

Abstract: In this paper, we studied the vibration performance, energy transfer and stability of the offshore wind turbine tower system under mixed excitations. The method of multiple scales is utilized to calculate the approximate solutions of wind turbine system. The proportional-derivative controller was applied for reducing the oscillations of the controlled system. Adding the controller to single degree of freedom system equation is responsible for energy transfers in offshore wind turbine tower system. The steady state solution of stability at worst resonance cases is studied and examined. The offshore wind turbine system behavior was studied numerically at its different parameters values. Furthermore, the response and numerical results were obtained and discussed. The stability is also analyzed using technique of phase plane and equations of frequency response. In addition, the numerical results and comparison between analytical and numerical solutions were obtained with MAPLE and MATLAB algorithms.

Keywords: Vibration control, stability, offshore wind turbine system, energy transfer.

1 Introduction

During the most recent decades, the interest of world energy is constantly increasing on worldwide scale. Renewable energy become a standard subject of these investigations. Wind energy production is one of the most cost efficient conservation projects [Silva, Arora and Brasil (2008); Shi, Han, Kim et al. (2015)]. The effect of the wave, wind and earthquake forces on dynamic behavior of wind turbine, Also the method of Rayleigh's energy and ANSYS FSI analysis are applied to obtain the dynamic effects of blades on the tower [Van der Woude and Narasimhan (2014)]. A comprehensive study is carried

¹ Department of Mathematics and Statistics, Faculty of Science, Taif University, Taif, PO Box 888, Saudi Arabia.

² Department of Physics and Engineering Mathematics, Faculty of Electronic Engineering, Menoufia University, Menouf, PO Box 32952, Egypt.

³ Department of Mechanical Engineering, College of Engineering, Taif University, Taif, PO Box 888, Saudi Arabia.

⁴ Department of Mechanical Engineering, Faculty of Engineering, Assiut University, Assiut, PO Box 71516, Egypt.

⁵ Department of Electrical Engineering, College of Engineering, Taif University, Taif, PO Box 888, Saudi Arabia.

* Corresponding Author: Y. S. Hamed. Email: eng_yaser_salah@yahoo.com.

Received: 29 July 2019; Accepted: 11 August 2019.

out for the effect of different parameters on the offshore wind turbine system behavior and responses of soil monopile tower system [Bisoi and Haldar (2014)]. The effective control approach based on an active observer of a standard model of large rotating wind turbines is studied [Shi and Patton (2015)]. Passive control technique is investigated for vibrations of spar and offshore wind turbine nacelle using tuned mass dampers [Nguyen Dinh and Basu (2015)]. The active control strategy effects is studied for a barge floating wind turbine type using a hybrid mass damper [Hu and He (2017)]. Mathematical analysis is studied for the dynamics of wind turbines with control and time scale simulations [Eisa, Stone and Wedeward (2018)]. An active control study to suppress the structural vibrations of wind turbines has been proposed [Fitzgerald, Sarkar and Staino (2018)]. The effect of seismic loads and environmental forces on the behavior of the offshore wind tower is performed with two different approaches [Dagli, Tuskan and Gokkus (2018)]. An analytical solutions, chaotic dynamics and stability of some systems under multi excitation forces such as a simply rectangular plate, MEMS gyroscope and a Cartesian manipulator systems are obtained and studied by Hamed et al. [Hamed (2014); Hamed, EL-Sayed and El-Zahar (2016); Hamed, Alharthi and AlKhathami (2018)]. The analysis detailed of some dynamical systems with different forces is founded in the books [Cartmell (1990); Nayfeh, and Balachandran (1995)]. In the present work, the PD controller was applied for reducing the oscillations of the controlled system and transfer the energy to the offshore wind turbine tower system. The stability at worst resonance cases is examined. Also, the offshore wind turbine system behavior was studied numerically at its different parameters values. In addition, the numerical results and comparison between analytical and numerical solutions were obtained.

2 Description of structure and governing equation of motion

The structural modal of wind turbine consists of hub, tower, blade and concentrated mass. The hub height of the wind turbine is 65 m with diameter 6 m, the blade length is 24 m and the tower carried the weight of the hub, nacelle, and the rotor blades which is 83,000 kg. The structural modal subjected to some external forces such as wind and wave forces (F_a, F_H) and earthquake force (F_{eqk}). The offshore wind turbine tower model is shown in Fig. 1.

The equation of motion of the single degree of freedom system is obtained from Dagli et al. [Dagli, Tuskan and Gokkus (2018)] and described by the following equations:

$$\ddot{x} + \varepsilon\mu\dot{x} + \omega^2x + \varepsilon\alpha \cos \pi t + \varepsilon F_a \sin \Omega t = \varepsilon F_H \cos \Omega t \left| \cos \Omega t \right| \quad (1)$$

The initial conditions of Eq. (1) are $x(0) = 0.01$, $\dot{x}(0) = 0.01$ with displacement x and derivatives \dot{x}, \ddot{x} , linear damping coefficient μ , small perturbation ε where $0 < \varepsilon \ll 1$, excitation wind and wave forces F_a, F_H , Earthquake force $F_{eqk} = \alpha \cos \pi t$ and natural frequency ω and excitation frequency Ω . Applying the proportional-derivative

(PD) controller to the motion equation of the controlled system, we get the modified normalized equation as follows:

$$\ddot{x} + \varepsilon\mu\dot{x} + \omega^2x + \varepsilon\alpha \cos \pi t + \varepsilon F_a \sin \Omega t = \varepsilon F_H \cos \Omega t \left| \cos \Omega t \right| - \varepsilon (px + d\dot{x}) \tag{2}$$

where $(px + d\dot{x})$ is the PD controller.

2.1 Perturbation analysis

Multi-scale disturbance technique (MSPT) [Nayfeh (1985); Nayfeh and Mook (1995)] is performed to obtain approximate solutions for Eq. (2). Assuming that the solution is in the form:

$$x(t; \varepsilon) = x_0(T_0, T_1, T_2) + \varepsilon x_1(T_0, T_1, T_2) + \varepsilon^2 x_2(T_0, T_1, T_2) + O(\varepsilon^3) \tag{3}$$

We presented the derivatives in the form:

$$\left. \begin{aligned} \frac{d}{dt} &= D_0 + \varepsilon D_1 + \varepsilon^2 D_2 + \dots \\ \frac{d^2}{dt^2} &= D_0^2 + 2\varepsilon D_0 D_1 + \varepsilon^2 (D_1^2 + 2D_0 D_2) + \dots \end{aligned} \right\} \tag{4}$$

The time scales $T_n = \varepsilon^n t$ and the derivatives $D_n = \partial/\partial T_n$ where (n=0, 1). Substituting Eqs. (3)-(4) into Eq. (2) and equating the coefficients of ε leads to:

$$(D_0^2 + \omega^2)x_0 = 0 \tag{5}$$

$$(D_0^2 + \omega^2)x_1 = -2D_0 D_1 x_0 - \mu D_0 x_0 - \alpha \cos \pi t - F_a \sin \Omega t + F_H \cos \Omega t \left| \cos \Omega t \right| - px_0 - dD_0 x_0 \tag{6}$$

$$(D_0^2 + \omega^2)x_2 = -D_1^2 x_0 - 2D_0 D_2 x_0 - 2D_0 D_1 x_1 - \mu D_1 x_0 - \mu D_0 x_1 - px_1 - dD_0 x_1 - dD_1 x_0 \tag{7}$$

The general solution of Eq. (5) has the form:

$$x_0 = A_0 \exp(i\omega T_0) + \bar{A}_0 \exp(-i\omega T_0) \tag{8}$$

where A_0 and \bar{A}_0 are complex functions in T_1, T_2 . Substituting Eq. (8) into Eq. (6), the following are obtained:

$$\begin{aligned} (D_0^2 + \omega^2)x_1 &= \left[-i\omega (2D_1 A_0 + \mu A_0 + dA_0) - pA_0 \right] \exp(i\omega T_0) \\ &+ \left[i\omega (2D_1 \bar{A}_0 + \mu \bar{A}_0 + d\bar{A}_0) - p\bar{A}_0 \right] \exp(-i\omega T_0) + \frac{iF_a}{2} (\exp(i\Omega T_0) - \exp(-i\Omega T_0)) \end{aligned}$$

$$+ \frac{F_H}{4} (\exp(2i\Omega T_0) + \exp(-2i\Omega T_0)) - \frac{\alpha}{2} (\exp(i\pi T_0) + \exp(-i\pi T_0)) + \frac{F_H}{2} \quad (9)$$

For the abounded solutions of Eq. (9), the coefficients of secular terms $\exp(\pm i\omega T_0)$ must be removed and the general solution of Eq. (9) should be in form:

$$\begin{aligned} x_1 = & A_1 \exp(i\omega T_0) + \overline{A_1} \exp(-i\omega T_0) + \frac{iF_a}{2(\omega^2 - \Omega^2)} (\exp(i\Omega T_0) - \exp(-i\Omega T_0)) \\ & + \frac{F_H}{4(\omega^2 - 4\Omega^2)} (\exp(2i\Omega T_0) + \exp(-2i\Omega T_0)) - \frac{\alpha}{2(\omega^2 - \pi^2)} (\exp(i\pi T_0) + \exp(-i\pi T_0)) \\ & + \frac{F_H}{\omega^2} \end{aligned} \quad (10)$$

where $A_1, \overline{A_1}$ are complex functions in T_1, T_2 . Substituting Eqs. (8) and (10) into Eq. (7) and removing the secular terms from Eq. (7), the solution to this equation is as follows:

$$\begin{aligned} x_2 = & A_2 \exp(i\omega T_0) + \frac{(ip - \Omega d - \Omega\mu)F_a}{2(\Omega^2 - \omega^2)^2} \exp(i\Omega T_0) + \frac{(p + 2i\Omega d + 2i\Omega\mu)F_H}{2(4\Omega^2 - \omega^2)^2} \exp(2i\Omega T_0) \\ & - \frac{(p + i\pi d + i\pi\mu)\alpha}{2(\pi^2 - \omega^2)^2} \exp(i\pi T_0) - \frac{pF_H}{2\omega^4} + cc \end{aligned} \quad (11)$$

where A_2 and H_i , ($i=1, 2, 3, 4$) are complex functions in T_1, T_2 and cc are referred to conjugate terms. The solution of Eq. (1) is presented by:

$$x(t; \varepsilon) = x_0(T_0, T_1, T_2) + \varepsilon x_1(T_0, T_1, T_2) + \varepsilon^2 x_2(T_0, T_1, T_2) + \dots + \varepsilon^n x_n(T_0, T_1, T_2) \quad \text{From}$$

the approximate solutions obtained, we extracted all the resonances and reported them as follows:

- (a) The primary resonance: $\Omega = \pm\omega$
- (b) The super-harmonic resonance: $\Omega = \pm \frac{\omega}{2}$.

2.2 Stability analysis of the steady state solution

To stability examination, the analysis is studied to the first approximation. The solution depends only on T_0, T_1 and the stability is analyzed and studied for the solution at the primary resonance $\Omega = \omega$. The detuning parameter σ is presented as:

$$\Omega = \omega + \varepsilon\sigma_1 \quad (12)$$

From Eq. (8) the secular terms are removed and the solvability conditions for the first approximation are presented as:

$$\left[-i\omega(2D_1A_0 + \mu A_0 + dA_0) - pA_0\right] \exp(i\omega T_0) + \frac{iF_a}{2} \exp(i\Omega T_0) \quad (13)$$

Substituting Eqs. (12) into (13) and eliminating the secular terms leads to solvability conditions for the first and second-order expansions as:

$$\left[-i\omega(2D_1A_0 + \mu A_0 + dA_0) - pA_0\right] + \frac{iF_a}{2} \exp(i\sigma_1 T_1) \quad (14)$$

Let's introduce the polar form as:

$$A_0 = \frac{1}{2} a(T_1) \exp(i\psi(T_1)) \quad (15)$$

where a and ψ are the amplitude and phase of the motion at the steady state. Using Eqs. (15) into (14) to obtain the imaginary and real parts, the following equations are obtained as follows:

$$a' = -\frac{\mu}{2} a - \frac{d}{2} a + \frac{F_a}{2\omega} \cos \theta \quad (16)$$

$$a\psi' = \frac{pa}{2\omega} + \frac{F_a}{2\omega} \sin \theta \quad (17)$$

where $\theta = \sigma_1 T_1 - \psi$. The steady state solution occur where $a' = \theta' = 0$, then the solutions at steady state can be obtained for Eqs. (16) and (17) as follows:

$$\frac{\mu}{2} a + \frac{d}{2} a = \frac{F_a}{2\omega} \cos \theta \quad (18)$$

$$a\sigma_1 - \frac{pa}{2\omega} = \frac{F_a}{2\omega} \sin \theta \quad (19)$$

By squaring both sides of Eqs. (18) and (19) and adding the results, we obtained the frequency response equation in the form:

$$\sigma_1^2 - \left(\frac{p}{\omega}\right) \sigma_1 + \left(\frac{\mu^2}{4} + \frac{d^2}{4} + \frac{p^2}{4\omega^2} + \frac{d\mu}{2} - \frac{F_a^2}{4a^2\omega^2}\right) = 0 \quad (20)$$

2.3 Stability of nonlinear solution

To examine the stability of the nonlinear solutions, we takes

$$a = a_0 + a_1(T_1) \quad \text{and} \quad \theta = \theta_0 + \theta_1(T_1) \quad (21)$$

where a_0, θ_0 and a_1, θ_1 are corresponding to the nonlinear solution and perturbation terms respectively, where a_1, θ_1 are small compared to a_0, θ_0 . Using Eq. (20) into Eqs. (16), (17) and putting $\cos \theta_1 = 1$ and $\sin \theta_1 = \theta_1$, then

$$(a'_0 + a'_1) = -(a_0 + a_1) \frac{\mu}{2} - (a_0 + a_1) \frac{d}{2} + \frac{F_a}{2\omega} (\cos \theta_0 - \theta_1 \sin \theta_0) \quad (22)$$

$$(a_0 + a_1)(\sigma_1 - (\theta'_0 + \theta'_1)) = -\frac{p}{2\omega}(a_0 + a_1) + \frac{F_a}{2\omega}(\sin \theta_0 + \theta_1 \cos \theta_0) \quad (23)$$

For the steady state the Eqs. (22) and (13) become:

$$a'_1 = \left(-\frac{\mu}{2} - \frac{d}{2}\right)a_1 - \left(\frac{F_a}{2\omega} \sin \theta_0\right)\theta_1 \quad (24)$$

$$\theta'_1 = \left(\frac{F_a}{2\omega a_0^2} \sin \theta_0\right)a_1 - \left(\frac{F_a}{2\omega a_0} \cos \theta_0\right)\theta_1 \quad (25)$$

The systems (24) and (25) can be expressed in a matrix form as follows

$$\begin{bmatrix} a'_1 \\ \theta'_1 \end{bmatrix} = \begin{bmatrix} \Gamma_{11} & \Gamma_{12} \\ \Gamma_{21} & \Gamma_{22} \end{bmatrix} \begin{bmatrix} a_1 \\ \theta_1 \end{bmatrix} \quad (26)$$

where a_1, θ_1 are real functions of T_1 .

The eigenvalues of the system (26) is

$$\begin{vmatrix} \Gamma_{11} - \lambda & \Gamma_{12} \\ \Gamma_{21} & \Gamma_{22} - \lambda \end{vmatrix} = 0 \quad (27)$$

i.e.,

$$\lambda^2 - [\Gamma_{11} + \Gamma_{22}]\lambda + \Gamma_{11}\Gamma_{22} - \Gamma_{12}\Gamma_{21} = 0 \quad (28)$$

$$\text{where } \Gamma_{11} = \left(-\frac{\mu}{2} - \frac{d}{2}\right), \quad \Gamma_{12} = -\left(\frac{F_a}{2\omega} \sin \theta_0\right), \quad \Gamma_{21} = \left(\frac{F_a}{2\omega a_0^2} \sin \theta_0\right),$$

$$\Gamma_{22} = -\left(\frac{F_a}{2\omega a_0} \cos \theta_0\right).$$

Using the criterion of Routh-Hurwitz, the necessary and sufficient conditions for the system to be stable that the real parts of all roots of Eq. (28) are negative.

3 Results and discussion

The Runge-Kutta algorithm of fourth order is used to find the analytic results numerically for the equation of motion (2). Also, we examined the stability of the controlled system using the frequency response function and the effects of some different parameters on the behavior of the controlled system are also studied. Finally, we compared the analytical results with the numerical ones.

3.1 System behavior without control

The System behavior is studied numerically at the obtaining resonance cases from Eqs. (10) and (11). The Eq. (2) is integrated numerically at the system parameters:

$\mu = 0.04$, $\alpha = 9.73$, $\Omega = \omega = 2.828$, $F_a = 67.17$, $F_H = 5.129$, $p = 15$, $d = 0.5$ Fig. 1, indicate the phase plane and time histories of uncontrolled offshore wind turbine tower system at primary condition $\Omega \cong \omega$. From this figure, we find that, the behavior of the uncontrolled system is nearly about 75% of the wind force F_a , 975% of the wave force F_H and phase plane showing multi limit cycle.

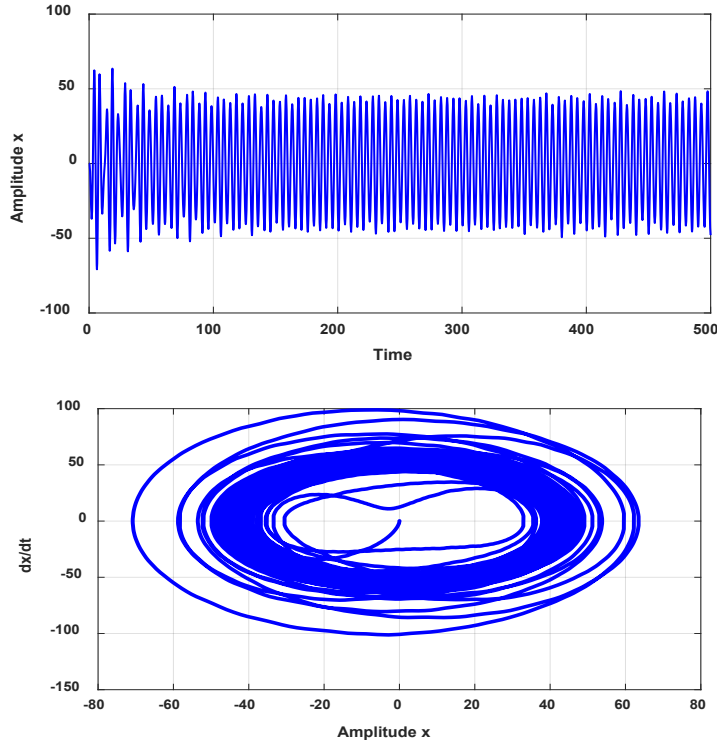


Figure 1: The amplitude and phase plane of the system without PD controller at primary resonance case $\Omega \cong \omega$

3.2 System behavior with control

Fig. 2 represent time histories for the offshore wind turbine tower system after applying the proportional-derivative (PD) controller at resonance case $\Omega \cong \omega$. In this figure, the amplitude for the controlled system is nearly 6% of the wind force F_a , 78% of the wave force F_H . Then, the efficiency of the controller E_a (uncontrolled system amplitude /controlled system amplitude) is about 12.5.

Figs. 3. and 4. show the transfer of energy between uncontrolled and controlled modes for the offshore wind turbine tower system due to values of wind, wave forces and super harmonic resonance case $\Omega \cong \frac{\omega}{2}$. From these figures, we observed that energy is

transferred from the uncontrolled system to the controlled system due to apply the PD controller with different values of wind and wave forces F_a , F_H and natural, excitation frequencies ω , Ω compared with its values in Fig. 1, so we can use these parameters to control the oscillation amplitude of the controlled system.

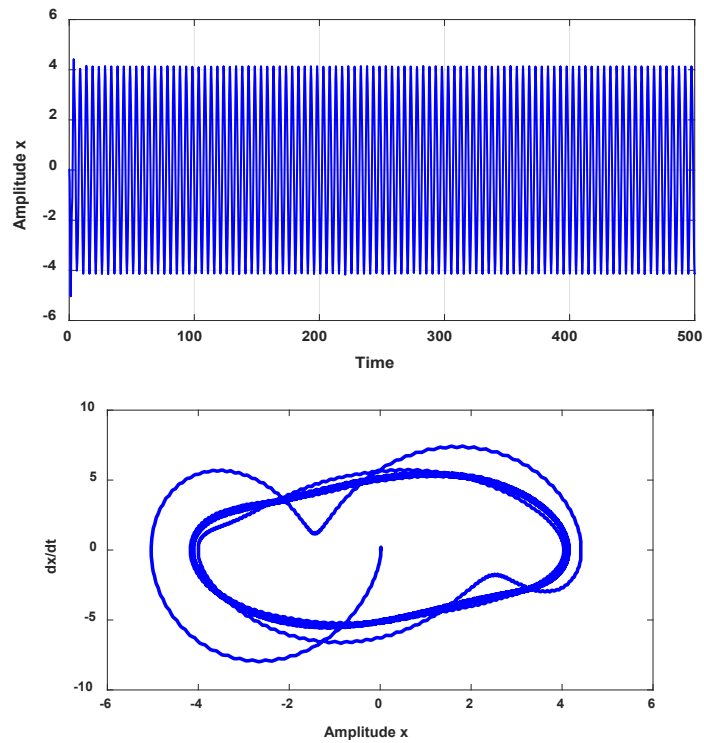


Figure 2: The amplitude and phase plane of the system with PD controller at primary resonance case $\Omega = \omega$

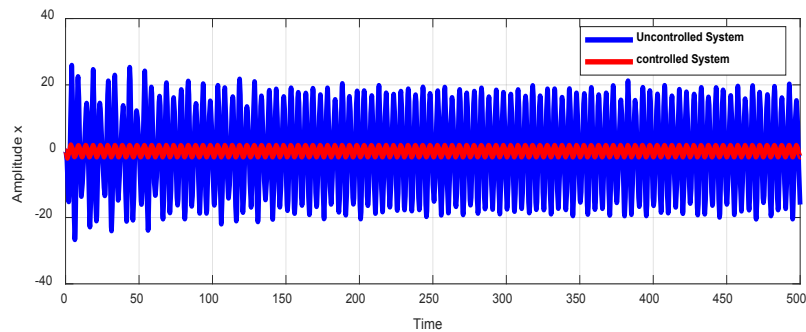


Figure 3: The energy transfer between uncontrolled and controlled system at $F_a = 27.56$, $F_H = 1.17$

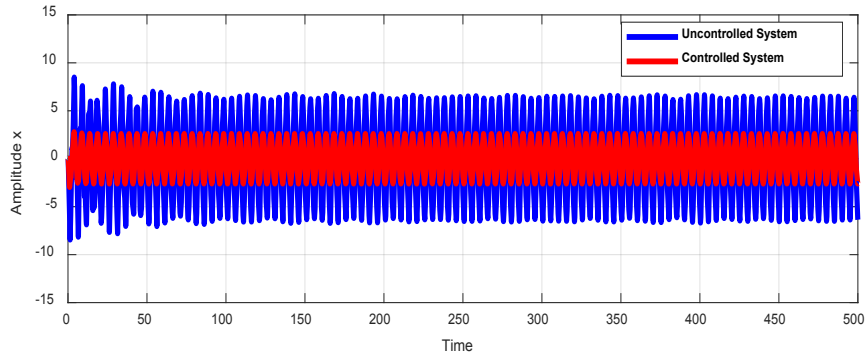


Figure 4: The energy transfer between uncontrolled and controlled system at $\Omega \approx \frac{\omega}{2}$

3.3 Response curves of the controlled system

In the section, we studied the different parameters effect and stability zone of the controlled system using frequency response curves. Also, using the numerical methods, the stability of nontrivial solutions is investigated for Eq. (20). In Fig. 5(a), the detuning parameter σ_1 effects on the behavior of the controlled system is shown. Figs. 5(b)-5(d) show that the behavior of the controlled system is a monotonic decreasing functions in the damping coefficient μ , the control parameter d and the natural frequency ω , also the curves of the system is shifted to right with increasing the values of the control parameter p as shown in Fig. 5(e). The behavior of the controlled system is a monotonic increasing function in the wind amplitude force F_a as shown in Fig. 5(f).

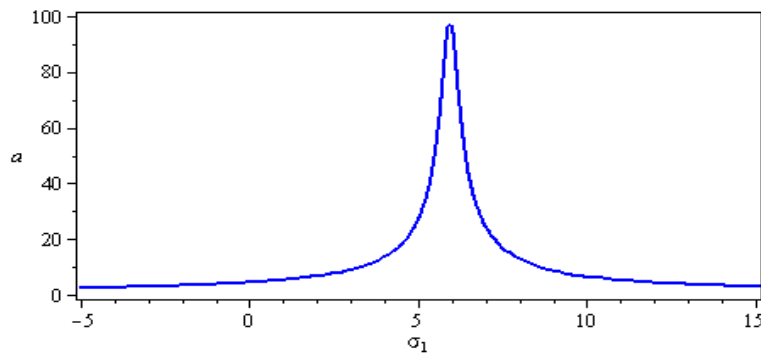


Figure 5(a): Effects of detuning parameter σ_1 on the system behavior

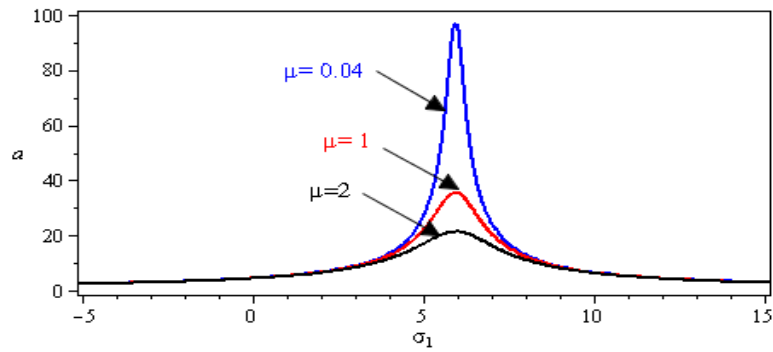


Figure 5(b): Effects of damping coefficient μ on the system behavior

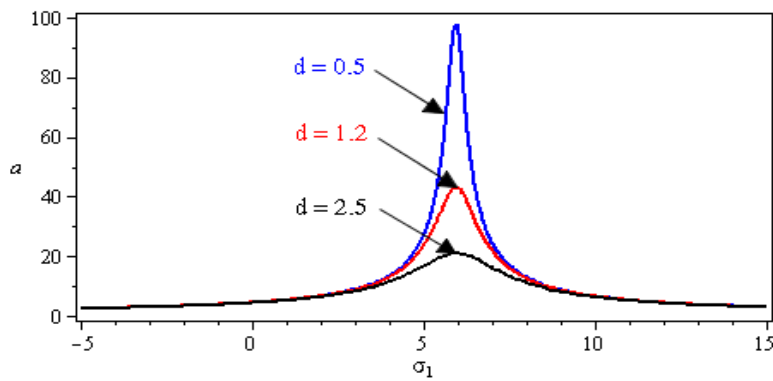


Figure 5(c): Effects of control parameter d on the system behavior

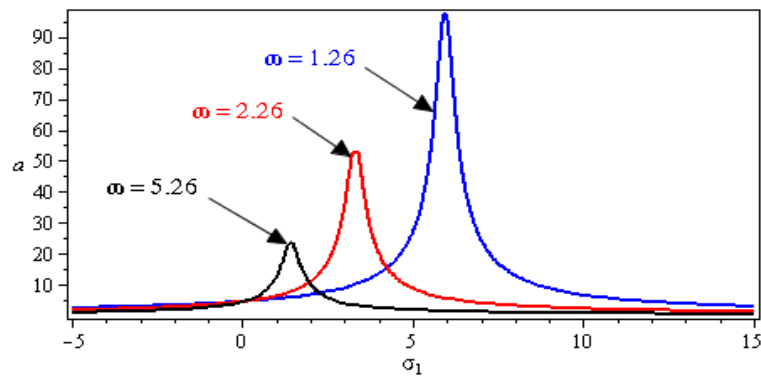


Figure 5(d): Effect of natural frequency ω on the system behavior

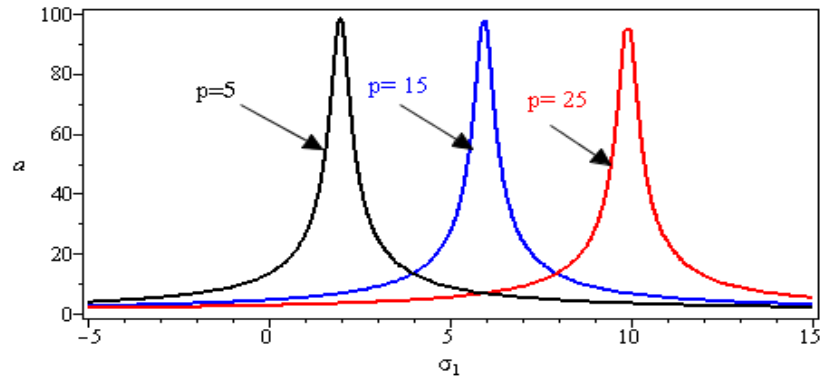


Figure 5(e): Effects of control parameter p on the system behavior

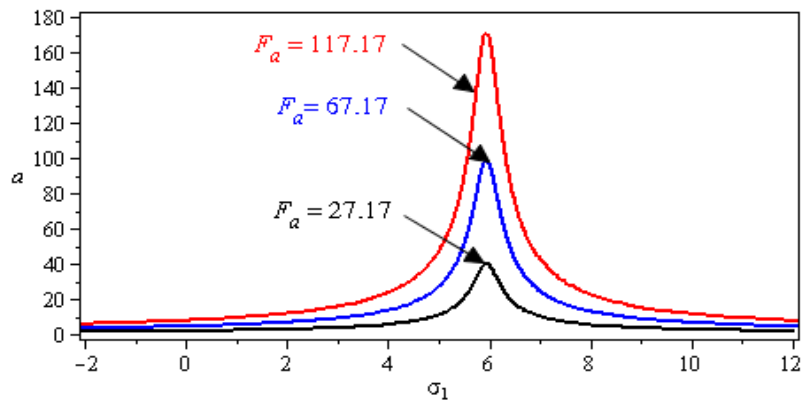


Figure 5(f): Effects of wind force F_a on the system behavior

3.4 Comparison of analytical and numerical simulation

In this subsection, the comparison of numerical simulation for the controlled system of Eq. (2) with perturbation solution of Eqs. (16) and (17) at different values of controller parameters p and d at primary resonance $\Omega = \omega$ is investigated as shown in Figs. 6-7. The red line indicates the solution of perturbation, while the blue line refers to numerical integration. In these figures, analytical results are well agreement with numerical simulation.

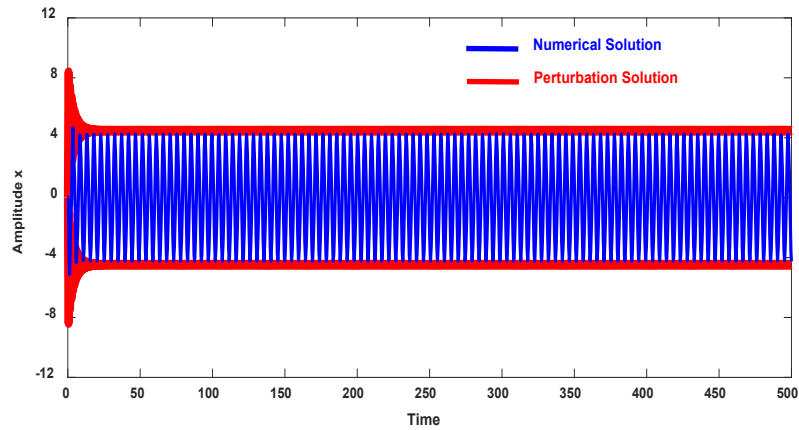


Figure 6: Comparison of analytical and numerical simulation of the system at $p = 15$, $d = 0.5$, $\Omega = \omega$

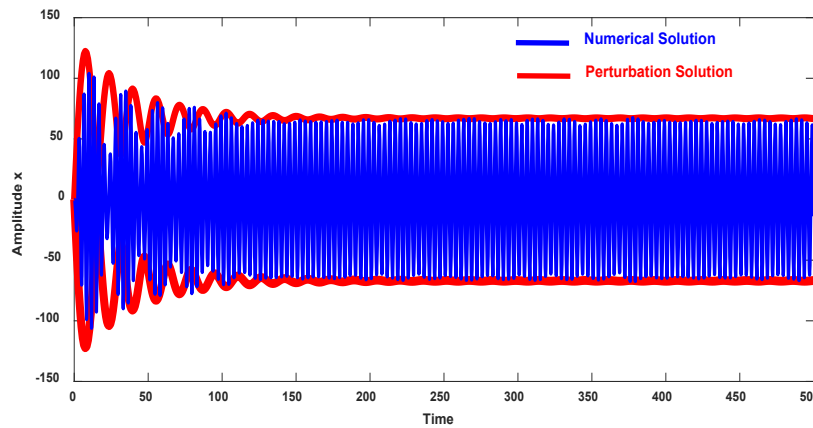


Figure 7: Comparison of analytical and numerical simulation of the system at $p = 1$, $d = 0.01$, $\Omega = \omega$

3.5 Comparison of numerical solution and response curve

Figs. 8-9 indicate a comparison of the system response with applying the PD controller at the parameters values used for stability at primary resonance $\Omega = \omega$. In these figures, the behavior of the controlled system is about 4 and 10 which is in a well agreement with the controlled system amplitude at $\sigma_1 = 0$.

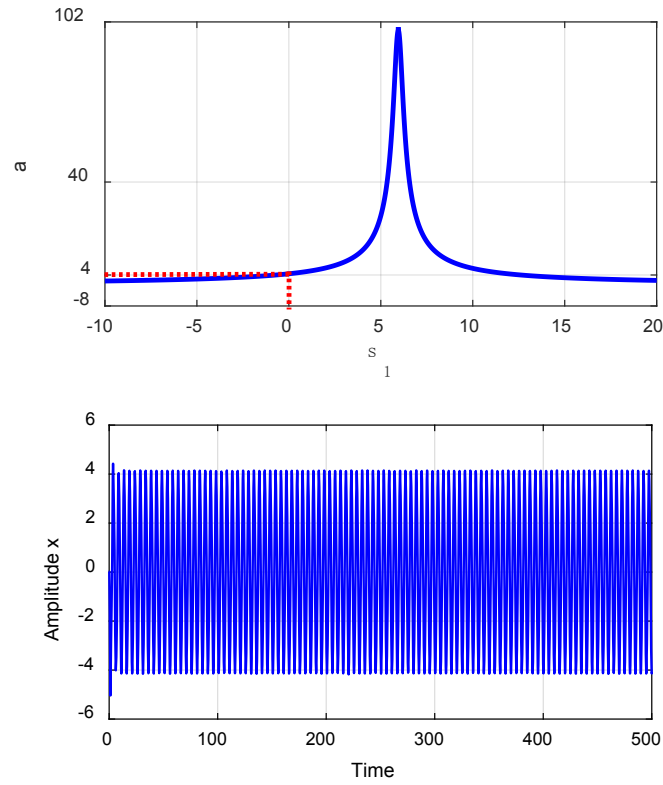
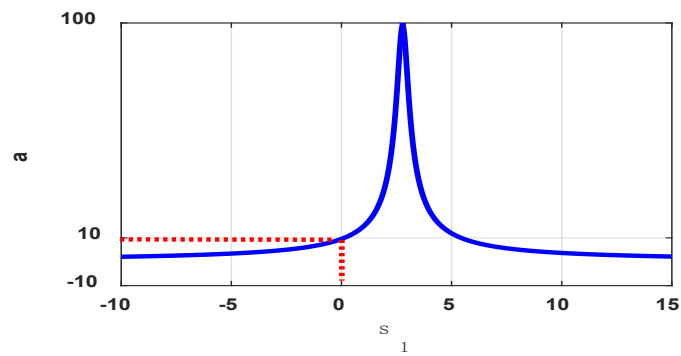


Figure 8: The response of the controlled system at the stability parameters values $p = 15$, $d = 0.5$, $\Omega = \omega$



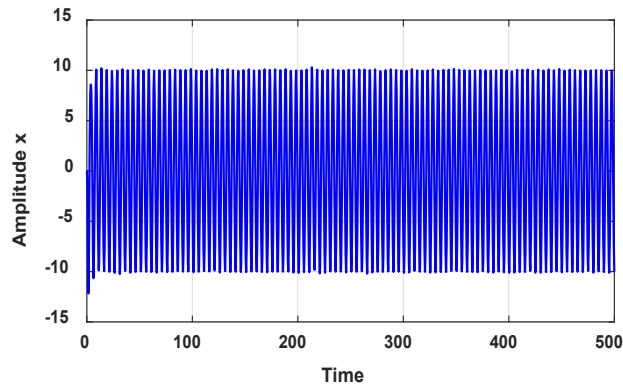


Figure 9: The response of the controlled system at the stability parameters values $p = 7$, $d = 0.5$, $\Omega = \omega$

4 Conclusions

The behavior of the offshore wind turbine system with mixed excitations and PD controller is investigated. The approximate solutions, stability analysis and numerical integration are studied for the system behavior. The different parameters effect and comparison of analytical with numerical solutions are studied numerically. From this study, we included the following:

1. The behavior of the uncontrolled system is nearly about 75% of the wind force F_a , 975% of the wave force F_H and the phase plane showing multi-limit cycle.
2. The amplitude for the controlled system is nearly 6% of the wind force F_a , 78% of the wave force F_H and the efficiency of the controller E_a is about 12.5.
3. The energy is transferred from the uncontrolled system to the controlled system due to apply the PD controller with different values of wind and wave forces F_a , F_H and natural, excitation frequencies ω , Ω .
4. The behavior of the controlled system is a monotonic decreasing functions in the damping coefficient μ , the control parameter d and the natural frequency ω .
5. The curves of the controlled system have a right shift to with increasing values of the control parameter p .
6. The behavior of the controlled system is a monotonic increasing function in the wind amplitude force F_a .
7. The analytical results are well agreement with numerical simulation

Acknowledgment: This work was supported by Taif University under research grant 1-439-6067. The authors would like to acknowledge the scientific support provided by the university.

Conflicts of Interest: The authors declare that they have no conflicts of interest.

References

- Bisoi, S.; Haldar, S.** (2014): Dynamic analysis of offshore wind turbine in clay considering soil-monopile-tower interaction, soil dynamics and earthquake. *Engineering*, vol. 63, pp. 19-35.
- Cartmell, M. P.** (1990): Introduction to linear, parametric and nonlinear vibrations. *Chapman & Hall, London*.
- Dagli, B. Y.; Tuskan, Y.; Gokkus, U.** (2018): Evaluation of offshore wind turbine tower dynamics with numerical analysis. *Advances in Civil Engineering*, vol. 2018, pp. 1-11.
- Eisa, S. A.; Stone, W.; Wedeward, K.** (2018): Mathematical analysis of wind turbines dynamics under control limits: boundedness, existence, uniqueness, and multi time scale simulations. *International Journal of Dynamics and Control*, vol. 6, pp. 929-949.
- Fitzgerald, B.; Sarkar, S.; Staino, A.** (2018): Improved reliability of wind turbine towers with active tuned mass dampers (ATMDs). *Journal of Sound and Vibration*, vol. 419, pp. 103-122.
- Hamed, Y. S.** (2014): Nonlinear oscillations and chaotic dynamics of a supported FGM rectangular plate system under mixed excitations. *Journal of Vibroengineering*, vol. 16, no. 7, pp. 3218-3235.
- Hamed, Y. S.; EL-Sayed, A. T.; El-Zahar, E. R.** (2016): On controlling the vibrations and energy transfer in MEMS gyroscopes system with simultaneous resonance. *Nonlinear Dynamics*, vol. 83, no. 3, pp. 1687-1704.
- Hamed, Y. S.; Alharthi, M. R.; AlKhathami, H. K.** (2018): Nonlinear vibration behavior and resonance of a Cartesian manipulator system carrying an intermediate end effector. *Nonlinear Dynamics*, vol. 91, pp. 1429-1442.
- Hu, Y.; He, E.** (2017): Active structural control of a floating wind turbine with a stroke-limited hybrid mass damper. *Journal of Sound and Vibration*, vol. 410, pp. 447-472.
- Nayfeh, A. H.** (1985): *Problems in Perturbation*. Wiley, New York.
- Nayfeh, A. H.; Balachandran, B.** (1995): *Applied Nonlinear Dynamics: Analytical, Computational and Experimental Methods*. Wiley, New York.
- Nayfeh, A. H.; Mook, D. T.** (1995): *Nonlinear Oscillations*. Wiley, New York.
- Nguyen Dinh, V.; Basu, B.** (2015): Passive control of floating offshore wind turbine nacelle and spar vibrations by multiple tuned mass dampers. *Structural Control and Health Monitoring*, vol. 22, pp. 152-176.
- Shi, F.; Patton, R.** (2015): An active fault tolerant control approach to an offshore wind turbine model. *Renewable Energy*, vol. 75, pp. 788-798.

Shi, W.; Han, J.; Kim, C.; Lee, D.; Shin, H. et al. (2015): Feasibility study of offshore wind turbine substructures for southwest offshore wind farm project in Korea. *Renewable Energy*, vol. 74, pp. 406-413.

Silva, M. A.; Arora, J. S.; Brasil, R. M. (2008): Formulations for the optimal design of RC wind turbine towers. *International Conference on Engineering Optimization, Rio de Janeiro, Brazil*.

Van der Woude, C.; Narasimhan, S. (2014): A study on vibration isolation for wind turbine structures. *Engineering Structures*, vol. 60, pp. 223-234.